Joint Detection and CFO Estimation for QAM Constellations

P. Pedrosa$^{(1,2)}$, R. Dinis$^{(1,3)}$ and F. Nunes$^{(1,2)}$
$^{(1)}$Instituto de Telecomunicações, 1049-001, Lisboa, Portugal
$^{(2)}$Instituto Superior Técnico, Universidade Técnica de Lisboa, 1049-001 Lisboa, Portugal
$^{(3)}$Faculdade de Ciências e Tecnologia, Universidade Nova de Lisboa, 2829-516 Caparica, Portugal
e-mail:{ppedrosa, rdinis, nunes}@lx.it.pt

***Abstract*—In this paper we propose the use of QAM constellations, specifically 4, 16, and 64-QAM, in severely time-dispersive channels and with moderate CFOs (Carrier Frequency Offsets). We consider an SC-FDE (Single Carrier Frequency-Domain Equalization) and assume that previously to the equalization procedure a coarse CFO estimation and compensation is performed. Since the coarse CFO estimate can have a significant error leading to a residual CFO we present and evaluate a receiver with joint detection and carrier synchronization in order to guarantee a good BER. We employ frequency-domain iterative DFE (Decision Feedback Equalization) receivers denoted by IB-DFE (Iterative Block-Decision Feedback Equalization), which are combined with a DD (Decision-Directed) CFO estimator. Our aim is to determine the synchronization requirements for 4, 16, and 64-QAM and compare several methods for the DD CFO estimators when using these QAM constellations.**[1]

***Index Terms*—Carrier frequency offset, single carrier frequency-domain equalization, quadrature amplitude modulation.**

I. Introduction

Due to an increased demand for wireless services, future systems are required to support high quality of service at high data rates. For such high data rates, the time-dispersion effects associated to the multipath propagation can be severe. In this case, conventional time-domain equalization schemes are not practical. Alternative techniques employing block transmission with appropriate cyclic extensions and employing FDE (Frequency-Domain Equalization) techniques have been shown to be suitable for high data rate transmission over severely time-dispersive channels without requiring complex receivers. Due to the inclusion of the cyclic prefix, the convolution inherent in the transmission of a block over a multipath fading channel is equivalent, in the frequency domain, to a product. The most popular modulations based on this latter concept are the OFDM (Orthogonal Frequency Division Multiplexing) modulations [1]. An alternative approach based on the same principle are block transmission SC modulations (Single Carrier) combined with FDE (also denoted SC-FDE) [2]. Both schemes have similar implementation complexities; nevertheless SC-FDE schemes require simpler receivers. In this paper we consider the SC-FDE approach.

A promising IFDE (Iterative FDE) technique for SC-FDE, denoted IB-DFE (Iterative Block-Decision Feedback Equalizer), was proposed in [3]. This technique was later extended to diversity scenarios and layered space-time schemes. These IFDE receivers can be regarded as iterative DFE (Decision Feedback equalizer) receivers with the feedforward and the feedback operations implemented in the frequency domain (see [4] and references therein). An IB-DFE receiver with joint post-equalization carrier frequency synchronization was proposed in [5]. This receiver can be regarded as a modified turbo equalization scheme where, for each iteration, we perform DD (Decision-directed) CFO (Carrier Frequency Offset) estimation.

Earlier IB-DFE implementations considered hard-decisions (weighted by the blockwise reliability) in the feedback loop. To improve the performance and allow truly turbo FDE implementations, IB-DFE schemes with soft decisions were proposed [6], [7], [8] usually only for QPSK constellations. The extension for larger constellations leads to difficulties on the computation of the reliability of each block, as well as problems on the computation of the average symbol values conditioned to the FDE and the channel decoder output.

In [9] SC-FDE schemes with IB-DFE receivers were considered and a general method for the computation of the receiver parameters for any constellation was proposed. The approach relies on an analytical characterization of the mapping rule where the constellation symbols are written as a linear function of the transmitted bits. This method is then employed in both uniform and non-uniform QAM constellations. We will use these results to implement a joint IB-DFE with carrier frequency offset synchronization for QAM constellations.

To maintain high power and spectral efficiencies, the cyclic extension, which has to be longer than the overall channel impulse response length, must be a small fraction of the block duration. As a consequence, we usually need large blocks for severely time-dispersive channels, with hundreds or even thousands of symbols and, typically the frequency errors cannot exceed a small fraction of the inverse of the block duration. This means that we have higher sensitivity to frequency errors for larger blocks, making accurate carrier

[1]This work was partially supported by the FCT–Fundação para a Ciência e Tecnologia (pluriannual funding, ADCOD project PTDC/EEA-TEL/099973/2008, U-BOAT project PTDC/EEA-TEL/67066/2006, and PhD grant SFRH/BD/40265/2007).

synchronization mandatory. Frequency errors usually originate from the frequency mismatch between the oscillators at the transmitter and receiver. Another possible source of frequency errors is the Doppler frequency shift caused by relative motion between the transmitter and the receiver.

While discussing carrier synchronization, two synchronization levels have to be distinguished, namely, carrier phase and carrier frequency synchronization. Furthermore, depending on the magnitude of the carrier frequency offset two types of synchronization can be attained, namely, a coarse synchronization and a fine synchronization. Usually, algorithms for fine synchronization require some type of previous coarse frequency estimation. Typically, fine carrier frequency synchronization systems are designed to deal with frequency offsets less than 10% of the symbol duration. Also, based on the degree of knowledge that the receiver has on the transmitted signal, these systems can be separated into three categories: data-aided (DA); non-data aided (NDA); and decision-directed (DD) (see [10] and references therein).

The major contribution of this paper is to compare four different methods for the DD CFO estimator and present the synchronization requirements for 4, 16, and 64-QAM. The comparison of the different methods is made by resorting to the BER performance. The study of the synchronization requirements is carried out by presenting the linearity range for a noiseless channel with residual CFO and for a frequency selective channel with low noise and residual CFO and also by presenting the impact of CFO on the BER performance of 16, and 64-QAM for a frequency-selective channel. Some assumptions are made: notably, perfect channel estimation and timing synchronization.

II. System description

A. Mapping Rules

Assume the transmitted symbols s_n belong to a given alphabet $\mathcal{G}$ (i.e. a given constellation) with dimension $M = \#\mathcal{G}$ and are selected according to the corresponding bits $\beta_n^{(m)}$, $m = 1, 2, \ldots, \mu$ $\left(\mu = \log_2(M)\right)$. i.e., $s_n = f\left(b_n^{(1)}, b_n^{(2)}, \ldots, b_n^{(\mu)}\right)$, with $b_n^{(m)} = 2\beta_n^{(m)} - 1$. We assume that $\beta_n^{(m)}$ is the mth bit associated to the nth symbol and $b_n^{(m)}$ is the corresponding polar representation, i.e., $\beta_n^{(m)} = 0$ or 1 and $b_n^{(m)} = -1$ or $+1$, respectively.

For 4-PAM constellations and Gray mapping it can be shown that the transmitted symbol is given by [9]

$$s_n = 2b_n^{(2)} + b_n^{(1)} b_n^{(2)}, \tag{1}$$

whereas for 8-PAM constellations and Gray mapping we have

$$s_n = 4b_n^{(3)} + 2b_n^{(3)} b_n^{(2)} + b_n^{(3)} b_n^{(2)} b_n^{(1)}. \tag{2}$$

If the transmitted symbols are selected from a QAM constellation under a Gray mapping rule the M-QAM constellation is written as the sum of two PAM constellations each with dimension $\sqrt{M}$, one for the in-phase (real) component and the other for the quadrature (imaginary) component. Therefore, the corresponding mapping for M-QAM is straightforward: half of the bits are used to define the in-phase component and the other half is used to define the quadrature component. As a result, for 16-QAM the transmitted bit is given by,

$$s_n = 2b_n^{(2)} + b_n^{(1)} b_n^{(2)} + j(2b_n^{(4)} + b_n^{(3)} b_n^{(4)}) \tag{3}$$

while for 64-QAM it is given by

$$\begin{aligned} s_n = {} & 4b_n^{(3)} + 2b_n^{(3)} b_n^{(2)} + b_n^{(3)} b_n^{(2)} b_n^{(1)} + \\ & + j(4b_n^{(6)} + 2b_n^{(6)} b_n^{(5)} + b_n^{(6)} b_n^{(5)} b_n^{(4)}) \end{aligned} \tag{4}$$

B. IB-DFE Receiver with Joint Carrier Synchronization

In this section the IB-DFE receiver with joint carrier synchronization presented in [11] (see Fig. 1) is adapted for general QAM constellations. The received time domain block, $\{y'_n;\, n = 0, 1, \ldots, N-1\}$, is passed to the frequency domain by a DFT operation, leading to the block $\{Y'_k;\, k = 0, 1, \ldots, N-1\}$, with $Y'_k = S'_k H_k + N_k$, where H_k and N_k denote the channel transfer function and the channel noise, respectively, for the kth subchannel. The block of frequency-domain symbols $\{S'_k;\, k = 0, 1, \ldots, N-1\}$ is the DFT of the transmitted time-domain block, $\{s'_n;\, n = 0, 1, \ldots, N-1\}$, with $s'_n = s_n \exp(j2\pi \Delta f n T/N)$, where s_n denotes the nth data symbol to be transmitted, selected from a given constellation (e.g. a QAM or a PSK constellation) and Δf is the CFO.

For a given iteration i, the frequency-domain samples at the output of the FDE are given by $\tilde{S}_k'^{(i)} = F_k^{(i)} Y'_k - B_k^{(i)} \bar{S}_k'^{(i-1)}$, where $\{F_k^{(i)};\, k = 0, 1, \ldots, N-1\}$ are the feedforward coefficients and $\{B_k^{(i)};\, k = 0, 1, \ldots, N-1\}$ are the feedback coefficients. $\{\bar{S}_k'^{(i-1)};\, k = 0, 1, \ldots, N-1\}$ denotes the DFT of the block of the time-domain average symbol values associated to the previous iteration, $\{\bar{s}_n'^{(i-1)};\, n = 0, 1, \ldots, N-1\}$.

To obtain the average symbol values conditioned to the FDE output, $\bar{s}_n$, we need to obtain the average bit values conditioned to the FDE output, $\bar{b}_n^{(m)}$. These are related to the corresponding log-likelihood ratio as follows: $\bar{b}_n^{(m)} = \tanh(\lambda_n^{(m)}/2)$; using mapping rules (1)-(4) we obtain $\bar{s}_n$, which for the first iteration is $\bar{s}_n = 0$.

The log-likelihood ratio of the mth bit of the nth transmitted symbol is given by [9]

$$\begin{aligned} \lambda_n^{(m)} &= \log\left(\frac{\Pr(\beta_n^{(m)} = 1)}{\Pr(\beta_n^{(m)} = 0)}\right) \\ &= \log\left(\frac{\sum_{s \in \Psi_1^{(m)}} \exp\left(-\frac{|\tilde{s}_n - s|^2}{2\sigma^2}\right)}{\sum_{s \in \Psi_0^{(m)}} \exp\left(-\frac{|\tilde{s}_n - s|^2}{2\sigma^2}\right)}\right) \end{aligned} \tag{5}$$

where $\Psi_1^{(m)}$ and $\Psi_0^{(m)}$ are the subsets of $\mathcal{G}$ where $\beta_n^{(m)} = 1$ or 0, respectively (clearly $\Psi_1^{(m)} \cup \Psi_0^{(m)} = \mathcal{G}$ and $\Psi_1^{(m)} \cap \Psi_0^{(m)} = \emptyset$).

It can be shown that the optimum feedback coefficients are [12], [3][2] $B_k^{(i)} = F_k^{(i)} H_k - 1$, and the feedforward coefficients

[2]contrarily to [12] and [3], we are considering normalized equalizers, i.e., $\sum_{k=0}^{N-1} F_k^{(i)} H_k = 1$

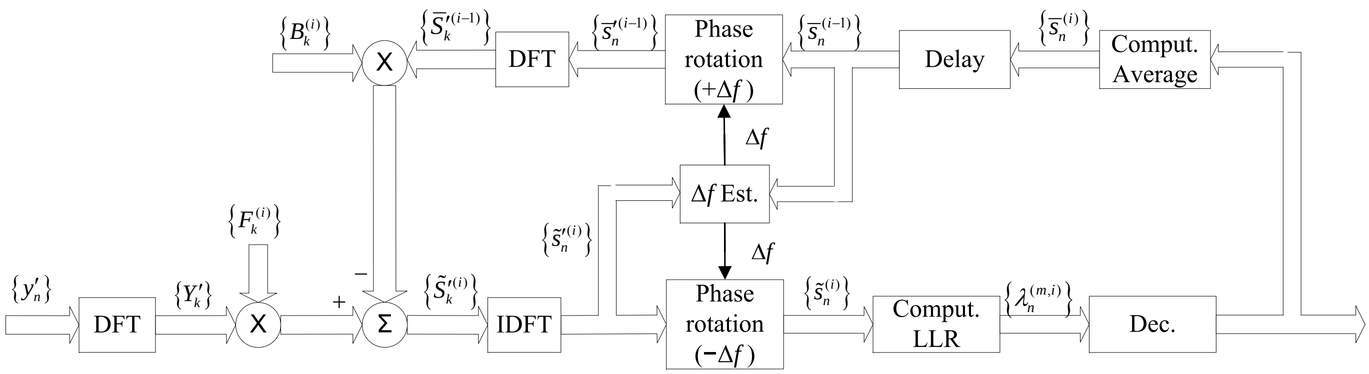

Fig. 1. Proposed receiver for joint equalization and carrier synchronization with soft decisions.

are given by $F_k^{(i)} = \breve{F}^{(i)}/\gamma^{(i)}$ with $\gamma^{(i)} = \frac{1}{N}\sum_{k=0}^{N-1} \breve{F}_k^{(i)} H_k$ and $\breve{F}_k^{(i)} = H_k^*/(\alpha + (1-(\rho^{(i-1)})^2)|H_k|^2)$, where $\alpha = \text{E}[|N_k|^2]/\text{E}[|S_k|^2]$ and the correlation factor (reliability of the estimates) $\rho^{(i-1)}$ is defined as $\rho^{(i-1)} = \text{E}[\hat{s}_n^{(i-1)} s_n^*]/\text{E}[|s_n|^2]$, where the block $\{\hat{s}_n^{(i-1)}; n = 0,1,\ldots,N-1\}$ denotes the data estimates associated to the previous iteration, i.e., the hard-decisions associated to the time-domain block at the output of the FDE, $\{\tilde{s}_n^{(i)}; n = 0,1,\ldots,N-1\} = \text{IDFT}\{\tilde{S}_k^{(i)}; k = 0,1,\ldots,N-1\}$.

C. Computation of the Correlation Factor

Finally the reliability of the estimates to be used in the feedback loop is given by

$$\rho = \frac{1}{2N}\sum_{n=0}^{N}\left(\rho_n^I + \rho_n^Q\right), \tag{6}$$

where ρ_n^I and ρ_n^Q can be regarded as the "reliabilities" of the real and imaginary parts of the nth symbol (i.e., the "reliabilities" of the "in-phase" and "quadrature" PAM parts of the QAM symbol). It can be shown that for 16-QAM we have [9]

$$\rho_n^I = \frac{2^2|\bar{b}_n^{(2)}| + 1^2|\bar{b}_n^{(2)}\bar{b}_n^{(1)}|}{2^2+1^2} \tag{7}$$

and

$$\rho_n^Q = \frac{2^2|\bar{b}_n^{(4)}| + 1^2|\bar{b}_n^{(4)}\bar{b}_n^{(3)}|}{2^2+1^2} \tag{8}$$

and for 64-QAM

$$\rho_n^I = \frac{4^2|\bar{b}_n^{(3)}| + 2^2|\bar{b}_n^{(3)}\bar{b}_n^{(2)}| + 1^2|\bar{b}_n^{(3)}\bar{b}_n^{(2)}\bar{b}_n^{(1)}|}{4^2+2^2+1^2} \tag{9}$$

and

$$\rho_n^Q = \frac{4^2|\bar{b}_n^{(6)}| + 2^2|\bar{b}_n^{(6)}\bar{b}_n^{(5)}| + 1^2|\bar{b}_n^{(6)}\bar{b}_n^{(5)}\bar{b}_n^{(4)}|}{4^2+2^2+1^2}. \tag{10}$$

For the first iteration, $\rho_n^I = \rho_n^Q = 0$.

D. CFO estimators

Several methods for the DD estimation of the carrier frequency offset can be implemented

$$\widehat{\Delta f} = \frac{N}{2\pi MT}\arg\{\xi\} \tag{11}$$

where ξ is for

Method I

$$\xi = \sum_{n=0}^{N-M-1} \frac{\tilde{s}_{n+M}'\tilde{s}_n'^*}{\bar{s}_{n+M}\bar{s}_n^*}; \tag{12}$$

Method II

$$\xi = \sum_{n=0}^{N-M-1} \tilde{s}_{n+M}'\tilde{s}_n'^*\bar{s}_{n+M}^*\bar{s}_n; \tag{13}$$

Method III

$$\xi = \sum_{n=0}^{N-M-1} \tilde{s}_{n+M}'\tilde{s}_n'^* e^{-j\arg(\bar{s}_{n+M})} e^{j\arg(\bar{s}_n)}; \tag{14}$$

Method IV

$$\xi = \sum_{n=0}^{N-M-1} \tilde{s}_{n+M}'\tilde{s}_n'^* \rho_{n+M} e^{-j\arg(\bar{s}_{n+M})} \rho_n e^{j\arg(\bar{s}_n)}. \tag{15}$$

Methods I and II are presented in [5] and [11], respectively. Methods III and IV are defined by the authors.

III. Performance Results

In this section we present a set of experimental results. We consider SC-FDE modulations with blocks of $N = 512$ "useful" modulation symbols (corresponding to a duration of $4\mu s$), plus an appropriate cyclic prefix. Additionally, we consider linear power amplification, perfect channel estimation and symbol synchronization. The propagation channel is characterized by the power delay profile type C for HIPERLAN/2 (HIgh PERformance Local Area Network) [13], with uncorrelated Rayleigh fading on different paths (similar results could be obtained for other severely time dispersive channel models with rich multipath propagation).

Fig. 2 depicts the impact of the CFO on the BER performance for 16-QAM. The values considered are $\Delta fT = 0$,

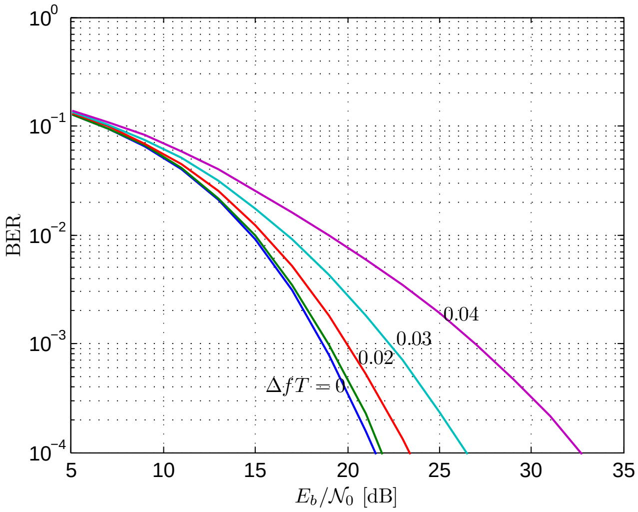

Fig. 2. Impact of the CFO on the BER performance for 16-QAM.

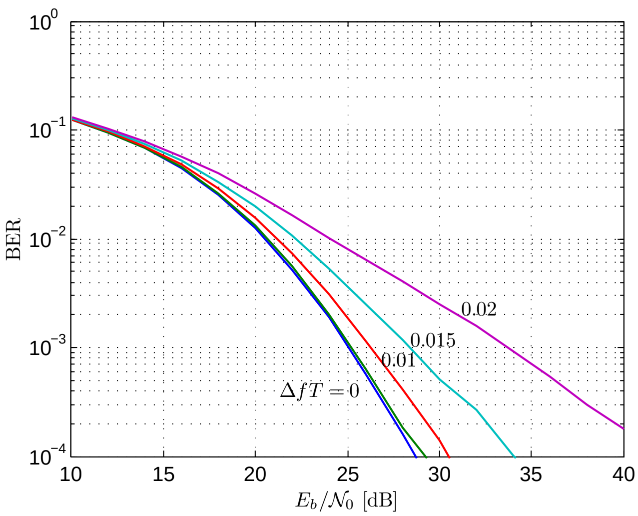

Fig. 3. Impact of the CFO on the BER performance for 64-QAM.

0.01, 0.02, 0.03, 0.04. We can observe an increased performance degradation as the values of the CFO rises. For $\Delta fT \leq 0.01$ we have an almost ideal performance and with $\Delta fT = 0.02$ we have about 2dB of degradation at $\text{BER} = 10^{-4}$.

Similarly to Fig. 2, Fig. 3 depicts the impact of the CFO on the BER performance for 64-QAM. The values considered are $\Delta fT = 0, 0.005, 0.01, 0.015, 0.02$. Again, we can observe an increased performance degradation as the values of the CFO grow. For $\Delta fT \leq 0.005$ we have an almost ideal performance and with $\Delta fT = 0.01$ we have about 2dB of degradation at $\text{BER} = 10^{-4}$.

Fig. 4 depicts the BER performance for the CFO estimation methods proposed in Sec. II-D. The results are obtained for different iteration orders, namely $i = \{1, 2, 5\}$. We consider a 16-QAM constellation and a CFO $\Delta fT = 0.03$. Inspecting the figure, we can see that Method I performs slightly worse

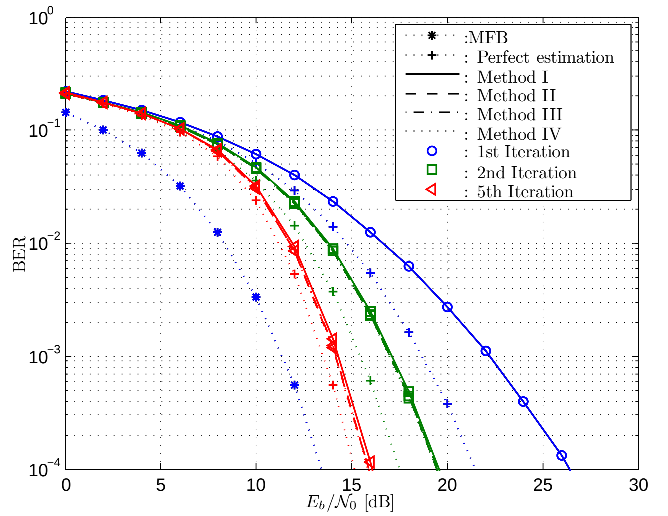

Fig. 4. Comparison of the BER performance for the proposed CFO estimation methods for 16-QAM and $\Delta fT = 0.03$.

that the other methods for the 5th iteration. Nevertheless, the difference is practically irrelevant. We see that with the joint equalization and CFO estimation the iterations produce progressively better results, not being far from the results with perfect estimation, i.e., with $\widehat{\Delta f} = \Delta f$. Note that there is a curve for the perfect estimator for each iteration, which are displayed at the immediate left side of the curves for the different methods. For comparison we also depicted the Matched Filter Bound (MFB), which is the best performance the system can achieve if no ISI is present [14], [12].

Similarly to Fig. 4, Fig. 5 depicts the BER performance for the CFO estimation methods proposed in Sec. II-D. For a 64-QAM constellation and a CFO $\Delta fT = 0.015$. The iteration orders on display are $i = \{1, 2, 5\}$. Again, and by inspection of the figure, we can see that Method I performs slightly worse than the other methods at the 5th iteration. As with 16-QAM, the difference is negligible. Again, the joint equalization and CFO estimation produces progressively better results not being far from the results with perfect estimation. Also depicted is the MFB for 64-QAM.

In Fig. 6 we plot

$$\widehat{\Delta f}T = \frac{N}{2\pi M} \arg\left\{ \sum_{n=0}^{N-M-1} s'_{n+M} s'^{*}_{n} \hat{s}^{*}_{n+M} \hat{s}_n \right\}, \qquad (16)$$

where $\{\hat{s}_n;\, n = 0, 1, \ldots, N-1\}$ are the hard decisions of $\{s'_n;\, n = 0, 1, \ldots, N-1\}$, versus ΔfT. The figure shows the values for which linearity is lost, i.e., the smallest ΔfT that introduces decision errors in the absence of channel noise. The curves are plotted for 4, 16 and 64-QAM. Also visible is the fact that the larger the constellations are the more sensitive to frequency errors they will be.

In Fig. 7 we plot $\widehat{\Delta f}T$ versus ΔfT, where $\widehat{\Delta f}T$ is given by (11), (12) with $E_b/\mathcal{N}_0 = 20$ dB. We can see that the slope of the straight segment of the curves is slightly biased. If we were to use lower values for $E_b/\mathcal{N}_0$ the bias would be more severe.

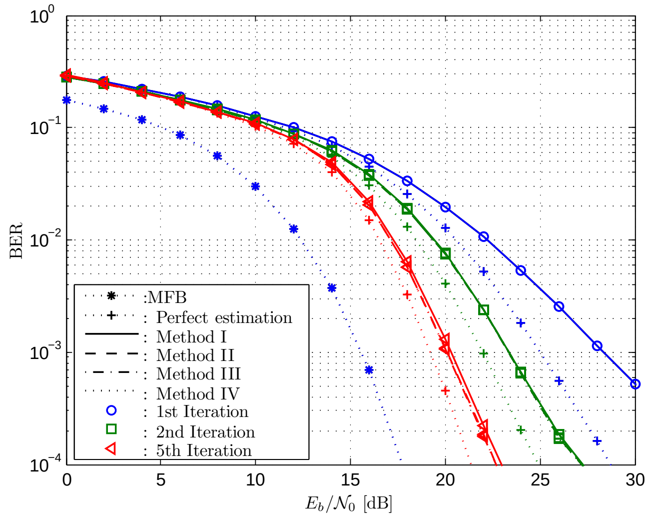

Fig. 5. Comparison of the BER performance for the proposed CFO estimation methods for 64-QAM and $\Delta fT = 0.015$.

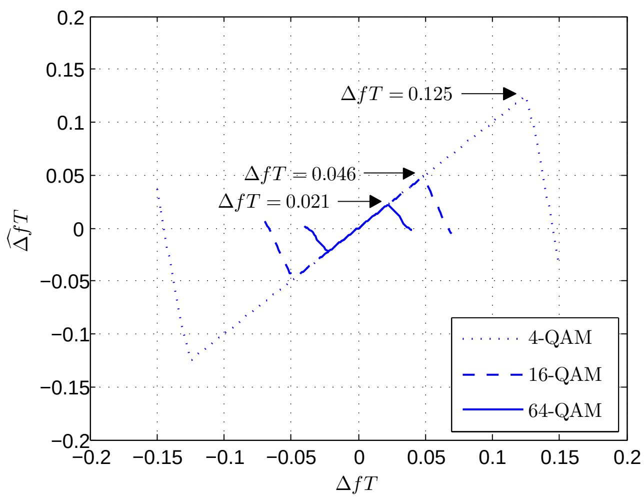

Fig. 6. Linearity range in the absence of noise.

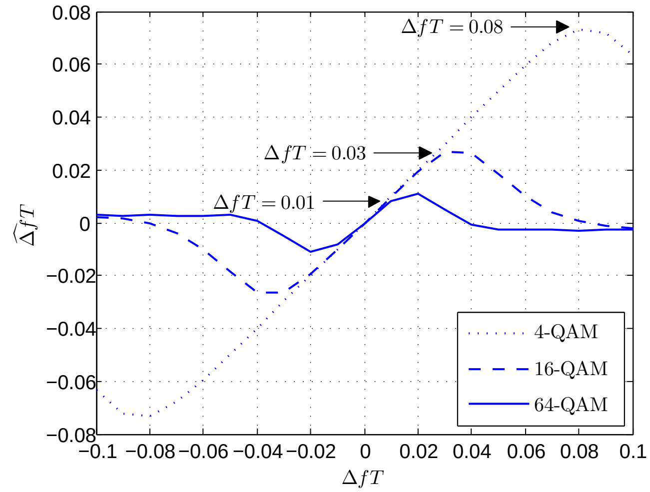

Fig. 7. Linearity range of Method I for a frequency-selective channel.

As in Fig. 6 we can see that larger constellations correspond to higher sensitivity to frequency errors. The results presented in Fig. 7 concern the 1st iteration of the DD CFO estimation and compensation procedure. The DD estimator (11), (12) is expected to produce more accurate CFO estimates as the iteration order increases.

IV. Conclusions

We compared several methods for the DD CFO estimator and determined the synchronization requirements for 4, 16, and 64-QAM. The comparison on the use of different methods for the DD CFO estimator revealed that there is little or no difference between them. On the other hand, the study on synchronization requirements revealed, unsurprisingly, that larger QAM constellations have more stringent synchronization requirements. Finally, under the stated assumptions, the joint IB-DFE with carrier synchronization revealed itself a powerful receiver, displaying a BER performance close to that of an IB-DFE with a perfect estimator and, for high iteration orders, near the MFB.

References

[1] L. Cimini Jr., "Analysis and simulation of a digital mobile channel using orthogonal frequency division multiplexing," *IEEE Trans. Commun.*, vol. 33, pp. 400–411, Jul. 1985.

[2] H. Sari, G. Karam, and I. Jeanclaude, "An analysis of orthogonal frequency-division multiplexing for mobile radio applications," in *Proc. IEEE Vehicular Technology Conference, (VTC'94)*, Stockholm, Jun. 1994, pp. 1635–1639.

[3] N. Benvenuto and S. Tomasin, "Block iterative DFE for single carrier modulation," *IEEE Electronic Letters*, vol. 39, no. 19, pp. 1144–1145, Sep. 2002.

[4] N. Benvenuto, R. Dinis, D. Falconer, and S. Tomasin, "Single carrier modulation with nonlinear frequency domain equalization: An idea whose time has come–again," *Proceedings of the IEEE*, vol. 98, no. 1, pp. 69–96, Jan. 2010.

[5] T. Araújo and R. Dinis, "Iterative equalization and carrier synchronization for single-carrier transmission over severe time-dispersive channels," in *Proc. IEEE Global Communications Conference (GLOBECOM'04)*, vol. 5, Dallas, Texas, USA, 29 Nov. - 3 Dec. 2004, pp. 3103–3107.

[6] N. Benvenuto and S. Tomasin, "Iterative design and detection of a dfe in the frequency domain," *Communications, IEEE Transactions on*, vol. 53, no. 11, pp. 1867–1875, Nov. 2005.

[7] A. Gusmao, P. Torres, R. Dinis, and N. Esteves, "A class of iterative FDE techniques for reduced-CP SC-based block transmission," in *Int. Symposium on Turbo Codes*, Apr. 2006.

[8] ——, "A turbo FDE technique for reduced-CP SC-based block transmission," vol. 55, no. 1, pp. 16–20, Jan. 2007.

[9] R. Dinis, P. Montezuma, N. Souto, and J. Silva, "Iterative frequency-domain equalization for general constellations," in *Sarnoff Symposium, 2010 IEEE*, Apr. 2010, pp. 1–5.

[10] C. Georghiades and E. Serpedin, *The handbook of communications*. CRC Press, 2002, ch. 19–Synchronization.

[11] R. Dinis, T. Araújo, P. Pedrosa, and F. Nunes, "Joint turbo equalization and carrier synchronization for SC-FDE schemes," *Euro. Trans. Telecomm.*, vol. 21, no. 2, pp. 131–141, Feb. 2010.

[12] R. Dinis, A. Gusmão, and N. Esteves, "On broadband block transmission over strongly frequency-selective fading channels," in *IEEE Wireless'03*, Calgary, Canada, Jul. 2003.

[13] ETSI, "Channel models for HIPERLAN/2 in different indoor scenarios," *ETSI EP BRAN 3ERI085B*, pp. 1–8, Mar. 1998.

[14] J. Proakis, *Digital Communications*, 4th ed. New York: McGraw-Hill, 2001.